Defence Science Journal, Vol. 74, No. 3, May 2024, pp. 381-388, DOI : 10.14429/dsj.74.19000

Determination of the Reserved Gap Between the Obturator Ring and the Breechblock in the Metallic Obturation Mechanism of a Large Caliber Gun Howitzer

Shukui Ding[#], Heng Wang[#] and Wenjie Qin[$,*]

[#]*China North Industries Corporation, Beijing - 100053, China*
[$]*Beijing Institute of Technology, Beijing - 100081, China*
[*]*E-mail: qinwj@bit.edu.cn*

ABSTRACT

A reserved gap between the obturator ring and the breechblock in the obturation mechanism of a large-caliber gun is required in the locked state of the gun, which is the main cause of gas leakage. In this study, the finite element analysis of the dynamic contact between the obturator ring and the breechblock and the computational fluid dynamics (CFD) analysis of the high-pressure gas flow through the gap between the obturator ring and the breechblock are conducted. The results show that the smaller the reserved gap is, the shorter the time period during which the contact pressure is zero after the obturator ring contacts with the breechblock will be under a low-bore pressure condition. The results also demonstrate that the leakage flow at the outlet of the gap and the gas flow in the external domain increase with the reserved gap size, and the gas flow in the external domain decays rapidly if the reserved gap is less than or equal to 0.02 mm under a high bore pressure condition. Based on the simulation results, the appropriate reserved gap value is determined and adopted in the studied gun, and good results are achieved in the firing tests.

Keywords: Sealing; Obturator mechanism; Large caliber gun howitzer; Finite element analysis; CFD

NOMENCLATURE

k	: Turbulent kinetic energy(m^2/s^2)
l	: Height of the gap (m)
M_ω	: Molecular weight (kg)
n	: Number of the grids at the outlet of the gap
p	: Static pressure (Pa)
p_{op}	: Working pressure (Pa)
P_k	: Effective production rate of k ($kg/(m\cdot s^3)$)
P_ω	: Production rate of ω ($kg/(m^3\cdot s^2)$)
R	: Ideal gas state constant (J/(mol·K))
S	: Leakage flow (kg/(m·s))
T	: Temperature (K)
U	: Incident free-stream flow velocity (m/s)
v_i	: Flow velocity of gas at grid i (m/s)
x_i	: Height of grid i (m)
β,β^*	: Turbulence modeling constant
μ	: Dynamic viscosity (m^2/s)
μ_t	: Modified eddy (or turbulent) viscosity (kg/(m·s))
ρ	: Density of fluid (kg/m^3)
ρ_i	: Density of gas at grid i (kg/m^3)
σ_k,σ_ω	: Diffusion constant
$\sigma_{\omega 2}$	: Diffusion constant related to the transformed k-ω model
ω	: Specific turbulent dissipation rate (1/s)

1. INTRODUCTION

The basic principle of gun launch is to use a high-pressure gas generated by the instantaneous detonation of gunpowder in a bore to throw a projectile along a certain trajectory. To achieve the range of a howitzer of more than 50 km, the muzzle velocity of a projectile needs to reach the value of approximately 900 m/s, and the bore pressure should be from 300 MPa to 400 MPa or even higher. Therefore, designing a reliable sealing obturation mechanism is crucial to achieving good gun performance.

As a large-caliber gun howitzer is considered in this study, the mixed obturation mode along the radial direction in the bore and along the end face outside the bore is employed, which has been widely used in howitzers[1]. The obturation along the end face refers to the seal between the obturator ring and the breechblock in the obturation mechanism. However, it is necessary to reserve an initial gap between the obturator ring and the breechblock to allow breechblock movement along the end face, which is the main cause of gas leakage in a gun. It can be inferred that the gas leakage is mainly related to the contact between the obturator ring and the breechblock and the flow of the gunpowder gas through the gap.

Since there have been fewer public studies on the sealing of the obturation mechanism, it has been necessary to learn from the research in other fields related to contact mechanics or hydrodynamics, or both. Murtagian, *et al.* investigated the influences of the contact pressure, seal length, load history, and other relevant factors on the effectiveness of metal-to-metal stationary seals through experiments and contact mechanics calculation and defined a sealability criterion for the metal-to-metal seal[2]. With the development of numerical

Received : 06 April 2023, Revised : 10 August 2023
Accepted : 14 November 2023, Online published : 10 May 2024

calculation methods, many studies have used the finite element method to analyze the sealing performance of structures by investigating the contact stresses at interfaces[3–8]. For instance, Zhang and Hu compared the mechanical properties and sealing performance of double-metal and single-metal sealing systems in roller cone bits and analyzed the effects of the compression ratio, fluid pressure, and thermal load on the contact stress distribution of a seal structure using the finite element method[3]. Some researchers used the computational fluid dynamics method to analyze sealing performance in view of the flow of sealed fluid[9–13]. Ledoux, *et al.* investigated the influence of surface defects on the static flat seal efficiency by computing the contact transmissivity using the Reynolds model for incompressible flow.[9] However, for a more comprehensive analysis, it is necessary to consider not only the contact but also the flow of the sealed fluid in sealing structures. Some scholars conducted analyses based on solid contact mechanics and fluid mechanics[14–16]. For instance, Ma, *et al.* studied the sealing performance of the new-generation single energizer metal seals through the thermal-fluid-solid coupling analysis; the sealing performance of the new-generation single energizer metal seals was investigated under different operating conditions and structural and material parameters[16]. Based on the results of the numerical simulations, the main design parameters affecting the sealing performance could be optimized.

In this paper, the determination of a reserved gap between an obturator ring and a breechblock in the studied obturation mechanism is considered, and the numerical simulations of a dynamic contact between the obturator ring and the breechblock

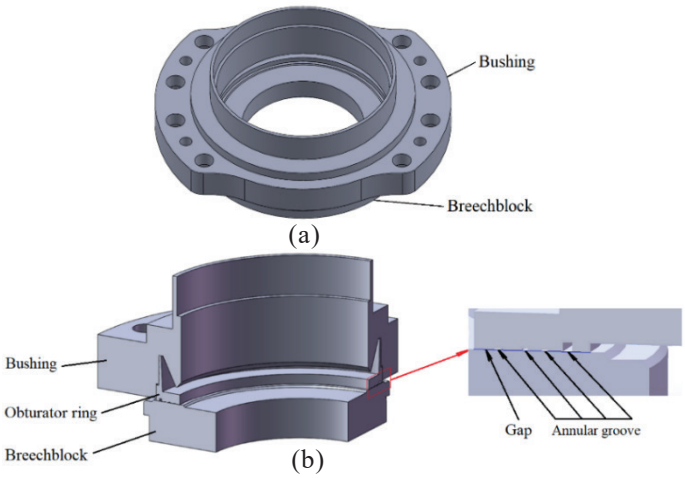

Figure 1. Geometry model of the obturator assembly: (a) Whole assembly and (b) Quarter of the assembly.

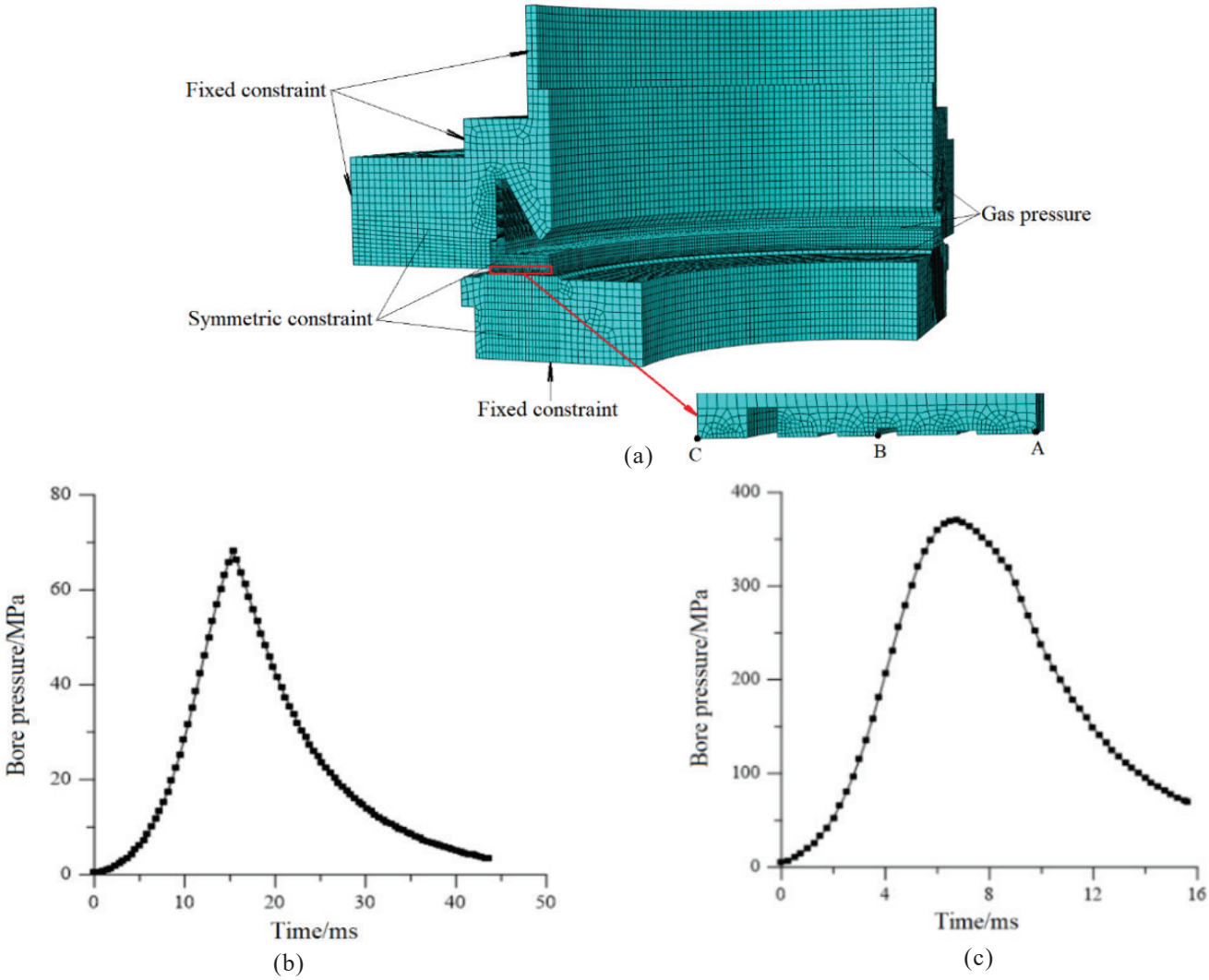

Figure 2. (a) Finite element model of the obturator assembly and bore pressures; (b) Low bore pressure and (c) High bore pressure.

and a high-pressure gas flowing through the gap between them are conducted. The influences of the dynamic contact of the seal parts and the flow of the gas passing through the time-varying gap on the sealing performance of the obturation mechanism are comprehensively analyzed. In particular, the gas flow in the external area out of the gap is simulated to investigate the effect of the reserved gap on the performance of the obturation mechanism, which has rarely been reported in the related literature. Based on the analysis results, an appropriate value of the reserved gap between the obturator ring and the breechblock in the studied gun is determined.

2. OBTURATION MECHANISM IN THE LARGE CALIBER GUN HOWITZER

The obturation mechanism of a large-caliber gun howitzer studied in this paper is composed of a bushing, an obturator ring, and a breechblock, and its three-dimensional geometric model is shown in Fig. 1(a). Considering the structural symmetry, the model of a quarter structure is constructed for the finite element contact analysis, as shown in Fig. 1(b). The obturator part in the obturation mechanism is a metal obturator ring. Its cylindrical surface of the front part is matched with the inner wall of a bushing, and its rear end face (i.e., the bottom surface) is perpendicular to its cylindrical surface. There is an initial gap between the bottom surface of the obturator ring and the top surface of the breechblock to allow the opening and closing movements of the breechblock, as presented in Fig. 1(b). When a projectile is fired, the front cylindrical surface of the obturator ring will expand radially to fit with the inner wall of the bushing and achieve radial sealing. Meanwhile, the obturator ring will move axially to eliminate the reserved gap and then will achieve end face sealing under the action of the gunpowder gas pressure in the bore. To improve the sealing reliability, several annular grooves are set on the bottom surface of the obturator ring to form labyrinth seals.

3. FINITE ELEMENT ANALYSIS OF DYNAMIC CONTACT BETWEEN OBTURATOR RING AND BREECHBLOCK

3.1 Finite Element Model

In this study, Abaqus 6.14 was adopted for finite element dynamic contact analysis. The quarter model of an obturator assembly, shown in Fig. 1(b), was meshed by hexahedral elements. The element size at the groove of the obturator ring was 0.2 mm, and it gradually increased to 0.5 mm and then to 1.0 mm in other areas in this part. The element size selected for the regions with key contact surfaces was 1 mm, and a larger element size of 2 mm was used for other regions in the bushing and breechblock. The mesh size were verified by examining the convergence of the model. The obtained mesh model of the obturator assembly is shown in Fig. 2(a). The material of the obturator ring, bushing, and breechblock was high-strength gun steel with a mass density of 7.85 t/m^3. Because the yield limit of this material was very high (higher than 882 MPa[17]) compared to the stress values observed in the analysis, the material model was adopted as linear elastic, with an elastic modulus value of 206 GPa and a Poisson's ratio of 0.27.

Fixed constraints were applied on the outer cylindrical surface of the bushing and the bottom of the breechblock, and symmetric constraints were applied on symmetrical planes of the quarter model. Friction contacts were defined between the inner surface of the bushing and the outer cylindrical surface of the obturator ring, as well as between the top surface of the breechblock and the bottom surface of the obturator ring. Further, the Coulomb friction model was adopted for the contacts, and the friction coefficient was set to 0.12. The dynamic gas pressure generated by the gunpowder detonation was applied to all the inner surfaces of the obturator assembly, including the gap. In this study, two bore pressures, namely a low bore pressure at a low projectile-launching speed and a high bore pressure at a high projectile-launching speed, are considered, as shown in Figs. 2(b) and 2(c), respectively.

3.2 Finite Element Analysis Results and Discussion

By using the previously established model, the transient dynamics analysis was conducted, and the obtained results are presented in Fig. 3.

3.2.1 Low Bore Pressure Condition

There is a reserved gap between the obturator ring and the breechblock, as shown in Fig. 1(b). Driven by the gas pressure in the gun bore, the obturator ring moves to contact with the breechblock to achieve sealing. When the gas pressure in the bore is low, the contact between the obturator ring and the breechblock might not be tight enough. Therefore, the dynamic contact pressure, representing the normal contact stress, between the obturator ring and the breechblock was investigated. It was found that the obturator ring would rebound in the initial contact stage; namely, the contact pressure value would become zero after the obturator ring contacted with the breechblock. For the reserved gap of 0.02 mm, the distributions of the contact pressure on the breechblock at different times after the obturator ring contacted with the breechblock are shown in Fig. 3(a). It can be seen that the obturator ring began to contact with the breechblock 0.1 ms after the launch, and the contact pressure was zero at 0.12 ms and 0.16 ms. After that, as the gas pressure increased, the rebound no longer occurred, and the obturator ring and the breechblock were in close contact.

Table 1. Changes of contact pressure with time at points A, B and C

Time (ms)	Contact pressure (MPa)		
	Point A	Point B	Point C
0.1	1.859	0	0
0.11	5.45296	2.27854	1.66791
0.12	0	0	0.977345
0.13	0	0	0
0.14	6.39499	0	0
0.15	3.22203	0	0
0.16	0	0	0
0.17	0.0437504	0	0
0.18	1.62064	0.634733	0
0.19	0.316023	1.1168	0.443389
0.20	0.931178	0	0

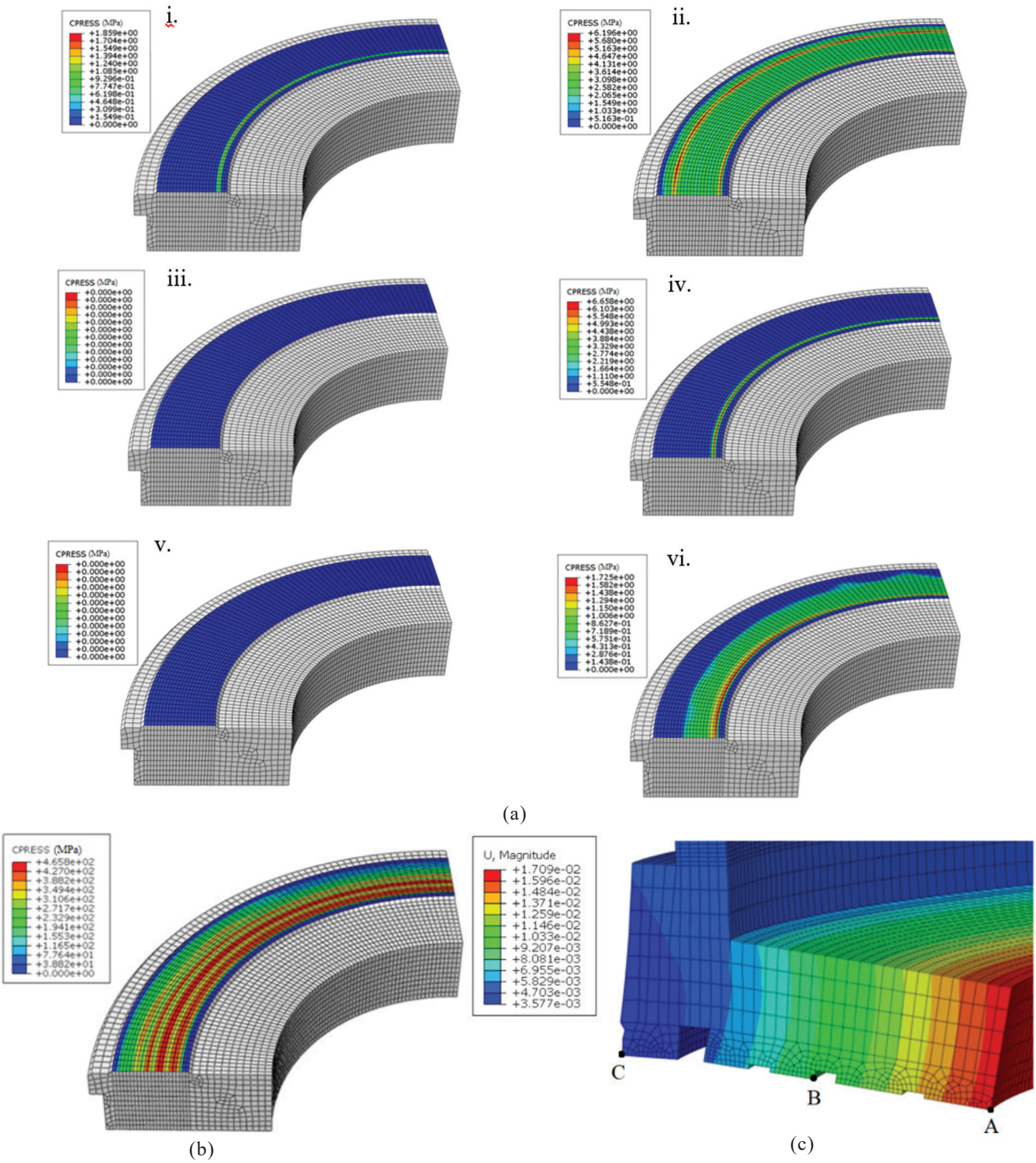

Figure 3. (a) Distributions of contact pressure on the breechblock at different times with the reserved gap of0.02mm: i. 0.10ms, ii. 0.11ms, iii. 0.12ms, iv. 0.14ms, v. 0.16ms, vi. 0.18ms; (b) Contact pressure on the breechblock when the bore pressure reaches its peak and (c) deformation of the obturator ring.

The time duration of the transient dynamic analysis was longer than 40 ms, but the time before the obturator ring was in stable contact with the breechblock was very short, less than 1 ms. Since this study investigated the rebound of the obturator ring, only the results before the obturator ring and the breechblock were in stable contact were considered. The changes in the contact pressure with time at points A, B, and C on the bottom surface of the obturator ring (see Fig. 2(a)) at the initial stage of the contact between the obturator ring and the breechblock with the reserved gap of 0.02 mm are presented in Table 1. It can be seen that the time period during which the contact pressure on the bottom surface of the obturator ring was

zero increased from the inside out. Accordingly, the rebound duration at point A was the shortest. When the reserved gap was set to 0.01 mm, 0.02 mm, 0.03 mm, 0.04 mm, and 0.05 mm, in turn, the behavior was similar, and the rebound duration at point A increased with the reserved gap size.

3.2.2 High Bore Pressure Condition

The results of the finite element simulation at the high-pressure condition showed that the bottom surface of the obturator ring kept contact pressure after it made the first contact with the breechblock, which indicated there were no rebound effects as under the low-pressure condition. When the bore pressure reached its peak value, the contact pressure on the breechblock also had its maximum value of 466 MPa, as shown in Fig. 3(b); this pressure was higher than the bore pressure and could ensure sealing. Under this condition, the focus was on the leakage of the high-pressure gas from the gap before the obturator ring contacted with the breechblock. Therefore, the dynamic change in the distance between the obturator ring and the breechblock before they were in contact was investigated. Under the action of the gas pressure in the bore, the axial displacements of different points on the bottom surface of the obturator ring gradually decreased from the inside out due to the deformation, as shown in Fig. 3(c). Further, changes in the distance between the bottom surface of the obturator ring and the top surface of the breechblock at different locations were calculated. The changes in the distance at points A, B, and C on the bottom surface of the obturator ring before the obturator ring was in contact with the breechblock obtained for different reserved gap sizes are presented in Table 2. It should be noted that when the distance at a point was zero, the obturator ring was in contact with the breechblock at that point. From the inside out, point A contacted with the breechblock first among the three points, blocking the gas leakage. The results demonstrated that the larger the reserved gap size was, the later the contact occurred.

Table 2. Distances between the bottom surface of the obturator ring and the top surface of the breechblock at points A, B and C with different reserved gaps

Reserved gap (mm)	Time (ms)	Distance (mm)		
		Point A	Point B	Point C
0.01	0.0	0.01	0.01	0.01
	0.005	0.0086845	0.00916065	0.0096636
	0.01	0.0066648	0.00792554	0.0091614
	0.015	0.0018426	0.0052455	0.0081993
	0.02	0	0.00178853	0.006565
0.02	0	0.02	0.02	0.02
	0.01	0.0156048	0.0173524	0.018934
	0.02	0.0035899	0.01065605	0.016398
	0.03	0	0.002842	0.0096825
0.03	0	0.03	0.03	0.03
	0.01	0.02560477	0.0273524	0.028934
	0.02	0.0135899	0.02065605	0.026398
	0.03	0	0.0100932	0.0201864
0.04	0	0.04	0.04	0.04
	0.01	0.0356048	0.0373524	0.038934
	0.02	0.0235899	0.03065605	0.036398
	0.03	0.0037218	0.0188844	0.030658
	0.04	0	0.0070282	0.0181694
0.05	0	0.05	0.05	0.05
	0.01	0.0456048	0.0473524	0.048934
	0.02	0.0335899	0.04065605	0.046398
	0.03	0.0137218	0.0288844	0.040658
	0.04	0	0.0144316	0.0288404

4. COMPUTATIONAL FLUID DYNAMICS ANALYSIS OF GAS FLOW UNDER HIGH BORE PRESSURE CONDITION

4.1 Turbulence Model

The flow and leakage of a high-pressure gas through the gap between the obturator ring and the breechblock under a high bore pressure condition were investigated through the CFD analysis using ANSYS Fluent 2020R2 software considering different reserved gaps. The main equations of the flow include the continuity equation and Navier Stokes equation.Due to the large changes in the gas pressure in the gun bore, it was necessary to consider the turbulent flow and compressibility of the gas, so a *k*-ω SST (shear stress transport) turbulence model was adopted. This model comprises two equations[18, 19], one defining the turbulent kinetic energy*k*, and another defining the specific turbulent dissipation rate ω, which are respectively given by:

$$\frac{\partial(\rho k)}{\partial t}+\frac{\partial(\rho U_i k)}{\partial x_i}=P_k-\beta^*\rho\omega k + \frac{\partial}{\partial x_j}\left[(\mu+\frac{\mu_t}{\sigma_k})\frac{\partial k}{\partial x_j}\right], \quad (1)$$

$$\frac{\partial(\rho\omega)}{\partial t}+\frac{\partial(\rho U_i\omega)}{\partial x_i}=P_\omega-\beta\rho\omega^2+\frac{\partial}{\partial x_j}\left[(\mu+\frac{\mu_t}{\sigma_\omega})\frac{\partial\omega}{\partial x_j}\right] + 2\rho(1-F_1)\sigma_{\omega 2}\frac{1}{\omega}\frac{\partial k}{\partial x_j}\frac{\partial\omega}{\partial x_j}, \quad (2)$$

where ρ is the fluid density; U represents the incident free-stream flow velocity; P_k is the effective production rate of k; μ is the dynamic viscosity; μ_t is the modified eddy (or turbulent) viscosity; P_ω is the production rate of ω; F_1 denotes the blending function; β^* and β are the turbulence modeling constants; σ_k and σ_ω are the diffusion constants; $\sigma_{\omega 2}$ is the diffusion constant related to the transformed *k*-ω model.

The ideal compressible gas model was used to simulate a high-pressure gas in the bore, which was defined as follows:

$$\rho=\frac{p_{\text{op}}+p}{\frac{R}{M_{\grave{u}}}T}, \quad (3)$$

where, p_{op} is the working pressure, which represents the dynamic gas pressure relative to the static pressure; p is the static pressure; R is the ideal gas state constant; M_ω is the molecular weight; T is the temperature.

4.2 Fluid Domain Modeling

The fluid domain formed by the high pressure gas flowing through the gap between the obturator ring and the breechblock

can be divided into an internal domain and an external domain as shown in Fig. 4. Since the fluid domain is circumferentially consistent, considering the calculation efficiency and accuracy, a two-dimensional fluid domain was the constructed for the CFD analysis. The height of the internal fluid domain at each point is time-varying according to the distance change between the deformed bottom surface of the obturator ring and the top surface of the breechblock, as described in Section 3.2.2.

Different fluid domains were meshed with different grid sizes determined by the convergence analysis. The grid size at the gap between the obturator ring and the breechblock was set to 10^{-6} m, and the grid size at the annular hollows and in the external flow domain was set to 10^{-5} m. The meshes of the fluid domains were adjusted according to the time-varying height of the gap.The boundary conditions of the model related to the inlet pressure, which denoted the gas pressure in the bore changing with time (Fig. 2(c)), the outlet pressure, which represented the atmospheric pressure, and the normal temperature wall with a temperature of 298.15 K.

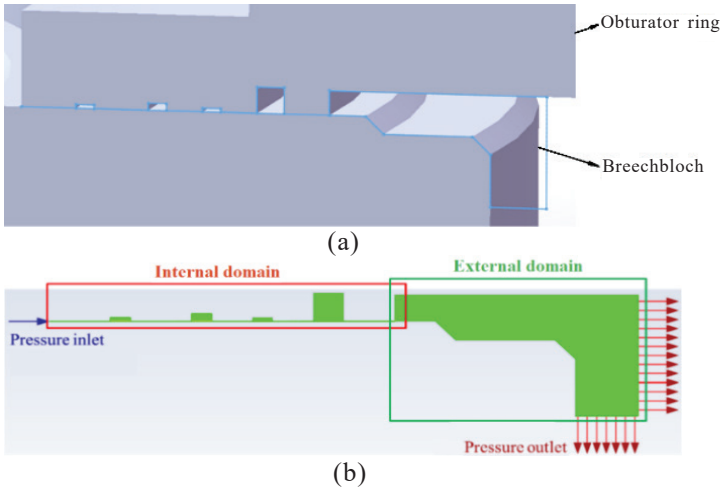

Figure 4. Model of the fluid domain: (a) Fluid domain; (b) Two-dimensional model.

4.3 CFD Analysis Results and Discussion

4.3.1 Gas Leakage Through the Gap

The gas leaking through the gap between the obturator ring and the breechblock was defined using the leakage flow S ($kg \cdot m^{-1} \cdot s^{-1}$) at the outlet of the gap, which can be expressed by:

$$S = \int_0^l \rho v \mathrm{d}x = \sum_{i=1}^{n} \rho_i v_i x_i \quad (4)$$

where, l (m) is the height of the gap between the obturator ring and the breechblock; n is the number of grids at the outlet; v_i ($m \cdot s^{-1}$) is the flow velocity of the gas at a grid i; ρ_i ($kg \cdot m^{-3}$) is the gas density at grid i; and x_i is the height of grid i.

The changes in the leakage flow at the outlet of the gap at several moments after launch and before the obturator ring contacted with the breechblock for different reserved gap sizes were obtained, as shown in Fig. 5. It can be seen that the leakage flow increased with the gap size at any time point, and the gas leakage flow reached the maximum value at the time of 0.01 ms. Before 0.01 ms, the leakage increased with the rapid increase in the gas pressure, although the gap gradually decreased. However, after 0.01 ms, the leakage decreased with

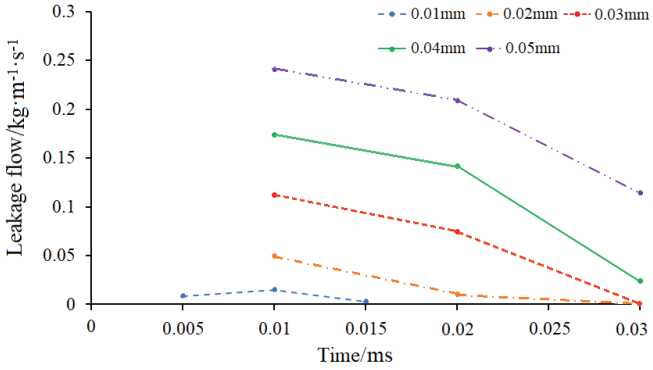

Figure 5. Changes of leakage flow with time with different reserved gaps.

the rapid decrease in the gap size, although the gas pressure increased.

4.3.2 Gas Flow in the External Domain

The leakage of a high-pressure gunpowder gas during the projectile launch will both affect the acceleration of the projectile and threaten the safety of operators. Therefore, the dynamic flow's behavior of the high-pressure gas in the external domain was investigated, and the gas velocity cloud diagrams at the time of 0.01 ms under different reserved gap sizes were determined, as shown in Fig. 6.

The results indicated that there was only a weak gas flow at the outlet of the gap when the reserved gap was 0.01 mm. When the reserved gap size was 0.02 mm, the flow of the gas in the external domain became obvious but decayed rapidly and almost disappeared at the outlet of the external domain. When the reserved gap size reached a value of 0.03 mm, there was an obvious jet phenomenon in the gas flow, and a Mach ring unique in the supersonic flow appeared at the outlet of the gap. The gas mainly flowed along the axial direction of the breechblock due to the wall obstruction. When the reserved gap size was 0.04 mm or 0.05 mm, the violent jet phenomena occurred in the gas flow, and the gas was ejected radially along the upper wall.

5. DETERMINATION OF RESERVED GAP BETWEEN OBTURATOR RING AND BREECHBLOCK

The results of the finite element analysis of the dynamic contact between the obturator ring and the breechblock showed that the smaller the reserved gap was, the shorter the time period during which the contact pressure was zero after the obturator ring contacted with the breechblock would be; thus, the better the sealing performance was under the condition of a low bore pressure. The results of the CFD analysis of the gas flowing through the gap showed that the smaller the reserved gap was, the smaller the leakage flow at the outlet of the gap was and the weaker the external leakage flow of the gas was under the condition of a high bore pressure. Considering that the launch frequency of a gun is relatively high (i.e., eight rounds per minute or even higher), a too-small reserved gap will hinder the operator from rapidly pulling or pushing the breechblock to open or close it. Further, the simulation results of the high-pressure gas flow in the external domain

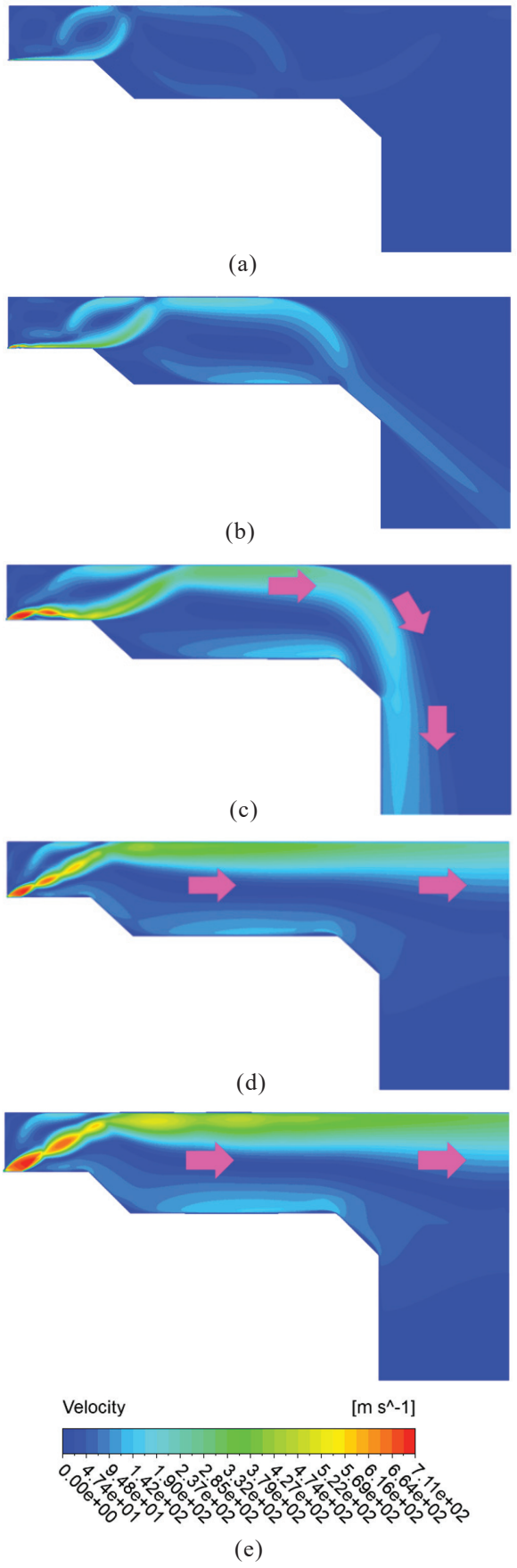

Figure 6. Gas velocity distributions in the external domain with different reserved gaps: (a) 0.01mm; (b) 0.02mm; (c) 0.03mm; (d) 0.04mm; (e) 0.05mm.

indicated that the flow of the gas decayed rapidly and did not pose a threat to the safety of operators when the reserved gap was less than or equal to 0.02 mm. Accordingly, the reserved gap of 0.02 mm should be appropriate for the gun considered in this study.

After the obturation mechanism was designed and processed for the reserved gap of 0.02 mm and applied to the gun for firing tests, it was found that the surface of the obturator ring after launch was in good condition. In the early stage, the reserved gap of 0.04 mm was adopted in the same gun, and the obturator ring was heavily eroded by the leakage gas after launch. Therefore, the reserved gap between the obturator ring and the breechblock in the obturation mechanism was finally set to 0.02 mm for the considered large-caliber gun howitzer.

6. CONCLUSION

This paper aims to determine an appropriate value of the reserved gap between the obturator ring and the breechblock in the obturation mechanism of a large caliber gun howitzer by performing the finite element analysis of dynamic contact between the obturator ring and the breechblock and the CFD analysis of the high-pressure gas flow through the gap between the obturator ring and the breechblock. The results of the dynamic contact analysis obtained using different reserved gap sizes show that under the condition of low bore pressure, the smaller the reserved gap is, the shorter the time period during which the contact pressure is zero after the obturator ring contacts with the breechblock is. The results also indicate that the phenomenon of the zero contact pressure on the whole bottom surface of the obturator ring after the obturator ring contacts with the breechblock does not occur under the condition of high bore pressure. In addition, the changes in the distance between the deformed bottom surface of the obturator ring and the top surface of the breechblock are calculated at different locations under this condition.

The CFD analysis results obtained under the high bore pressure condition show that the leakage flow at the outlet of the gap between the obturator ring and the breechblock and the gas flow in the external domain increase with the reserved gap size for any time point. The results also demonstrate that the flow of the gas in the external domain decays rapidly and does not pose a threat to the safety of operators if the reserved gap is less than or equal to 0.02 mm. Thus, the reserved gap of 0.02 mm is finally adopted in the gun considered in this study, and good results are achieved in the firing tests.

REFERENCES

1. Luo, Z.L.; Ru, Z.X.; Lu, T. & Zhang, Y. Obturation pattern analysis of high pressure wedge breechblock. *J. Gun Launch & Control*, 2006, 2, 21–24. doi: 10.3969/j.issn.1673-6524.2006.02.005
2. Murtagian, G.R.; Fanelli, V.; Villasante, J.A.; Johnson, D. H. & Ernst, H.A. Sealability of stationary metal-to-metal seals. *J. Tribol.*, 2004, **126**(3), 591–596. doi: 10.1115/1.1715103
3. Zhang, J. & Hu, Y. Mechanical behavior and sealing performance of metal sealing system in roller cone bits. *J. Mech. Sci. Technol.*, 2019, **33**(6), 2855–2862.

doi: 10.1007/s12206-019-0533-5
4. Zhou, Y.; Huang, Z.; Tan, L.; Ma., Y.; Qiu., C.; Zhang, F.; Yuan, Y.; Sun, C. & Guo, L. Cone bit bearing seal failure analysis based on the finite element analysis. *Eng. Fail. Anal.*, 2014, **45**, 292–299. doi: 10.1016/j.engfailanal.2014.07.007
5. Zhuang, Y.; Gao, L. X. & Yuan, P.B. Force analysis and tightening optimization of gas sealing drill pipe joints. *Eng. Fail. Anal.*, 2015, **58**, 173–183. doi: 10.1016/j.engfailanal.2015.08.032
6. Shen, M.; Peng, X.; Xie, L.; Meng, X. & Li, X. Deformation characteristics and sealing performance of metallic O-rings for a reactor pressure vessel. *Nucl. Eng. Techno.*, 2016, **48**, 533–544. doi: 10.1016/j.net.2015.11.009
7. Lei, D.Q.; Wang, Z.F. & Wang, Z.J. Effects of geometry and material properties on the residual stress of glass-to-metal seals in solar receiver tubes. *Energy Procedia*, 2014, **49**, 418–427. doi: 10.1016/j.egypro.2014.03.045
8. Qiao, L.; Keller, C.; Zencker, U. & Völzke, H. Three-dimensional finite element analysis of O-ring metal seals considering varying material properties and different seal diameters.*Int. J. Pres. Ves. Pip.*, 2019, **176**, 103953. doi: 10.1016/j.ijpvp.2019.103953
9. Ledoux, Y.; Lasseux, D.; Favreliere, H.; Samper, S. & Grandjean, J. On the dependence of static flat seal efficiency to surface defects. *Int. J. Pres. Ves. Pip.*, 2011, **88**, 518–529. doi: 10.1016/j.ijpvp.2011.06.002
10. Kim, S.; Kim, K. & Son, C. Three-dimensional unsteady simulation of a multistage axial compressor with labyrinth seals and its effects on overall performance and flow characteristics. *Aerosp. Sci. Technol.*, 2019, **86**, 683–693. doi: 10.1016/j.ast.2019.01.055
11. Zhang, W.; Wu, K.; Gu, C.; Tian, H.; Zhang, X. & Li, C. Swirl brakes optimization for rotordynamic performance improvement of labyrinth seals using computational fluid dynamics method. *Tribol. Int.*, 2021, **159**, 106990. doi: 10.1016/j.triboint.2021.106990
12. Zahorulko, A.V. & Lee, Y.B. Computational analysis for scallop seals with sickle grooves, part I: leakage performance. *Mech. Syst. Signal Pr.*, 2021, **147**, 107024. doi: 10.1016/j.ymssp.2020.107024
13. Zahorulko, A.V. & Lee, Y.B. Computational analysis for scallop seals with sickle grooves, part II: rotordynamic characteristics. *Mech. Syst. Signal Pr.*, 2021, **147**, 107154. doi: 10.1016/j.ymssp.2020.107154
14. Xiong, S. & Salant, R.F. A numerical model of a rock bit bearing seal. *Tribol. Trans.*, 2000, **43**(3), 542–548. doi: 10.1080/10402000008982375
15. Anwar, A.A.; Gorash, Y.; Dempster, W. & Hamilton, R. Literature research in relevant fields to understand pressure relief valve leak tightness in a static closed state. *Procedia Eng.*, 2015, **130**, 95–103. doi: 10.1016/j.proeng.2015.12.179
16. Ma, Y.; Yuan, Z.; Ni, Y.; Meng, X. & Peng X. Performance prediction and multi-objective optimization of metal seals in roller cone bits. *J. Petrol. Sci. Eng.*, 2022, **208**, 109316. doi: 10.1016/j.petrol.2021.109316
17. Wang, M.Q.; Dong, H.; Wang, Q.; Li, J.X. & Zhao, L. Microstructures and mechanical properties of high strength gun steels. *Ordnance Mater. Scie. Eng.*, 2003, **26**(2), 7–10, 18. doi: 10.3969/j.issn.1004-244X.2003.02.002
18. Menter, F.R. Two-equation eddy-viscosity turbulence models for engineering applications. *AIAA J.*, 1994, **32**(8), 1598–1605. doi:10.2514/3.12149
19. Costa Rocha, P. .; Barbosa Rocha, H.H.; Moura Carneiro, F.O.; Vieira da Silva, M.E. & Valente Bueno, A. *k–ω* SST (shear stress transport) turbulence model calibration: A case study on a small scale horizontal axis wind turbine. *Energy*, 2014, **65**, 412–418. doi: 10.1016/j.energy.2013.11.050

CONTRIBUTORS

Mr Shukui Ding graduated from Beijing Institute of Technology in 1983 and is currently a Chief Scientist of North Industries Corporation Group.
His contribution in the current study include: Planning the research, proposing methodology, collecting product data, and establishing computational model.

Dr Heng Wang obtained his PhD in Beijing Institute of Technology in 2005. His research focuses on the suppression weapon system, command and control weapon system and modern manufacturing technology etc.
His contribution in the current study include: Implementing the CFD analysis of the high pressure gas flow through the gap between the obturator ring and the breechblock in the obturation mechanism, reviewing and editing the manuscript.

Dr Wenjie Qin obtained her PhD from Beijing Institute of Technology. She has been on the faculty of the School of Mechanical Engineering in Beijing Institute of Technology. Her teaching and research focus on engineering design methods and simulation of mechanical systems.
Her contribution in the current study include: Conducting the finite element simulation of the dynamic contact process between the obturator ring and the breechblock in the obturation mechanism, and writing the original draft.